

## Coastal deformation in Lefkada Island associated with strong earthquake occurrence

V. KARAKOSTAS<sup>1</sup>, E. PAPADIMITRIOU<sup>1</sup>, P. PATIAS<sup>2</sup> and CH. GEORGIADIS<sup>3</sup>

<sup>1</sup> Geophysics Department, School of Geology, Aristotle University of Thessaloniki, Greece

<sup>2</sup> School of Rural & Surveying Engineering, Aristotle University of Thessaloniki, Greece

<sup>3</sup> School of Civil Engineering, Aristotle University of Thessaloniki, Greece

(Received: 13 November 2018; accepted: 22 January 2019)

**ABSTRACT** The Lefkada Island, central Ionian islands, Greece, deforms in response to rapid dextral strike-slip movement of the Cephalonia Transform Fault Zone accounted to 2-3 cm/yr. Historical and instrumental earthquakes had a major impact on the coastal landscape, as they had caused nearshore landslides, rockfalls, tsunami-induced flooding, and several centimetres coastal uplift and subsidence. Appreciable coseismic displacements were calculated at discrete points designating the coastlines after applying an elastic model and considering the coseismic slip of the 2003 ( $M$  6.3) and 2015 ( $M$  6.5) Lefkada earthquakes, and the 2014 Cephalonia Island doublet ( $M$  6.1 and  $M$  6.0), the latter being of negligible importance. Subsidence and uplift of several centimetres were calculated along the western Lefkada coastline, depending upon the position of the calculation point relative to the causative rupture and permanent localised uplift for certain areas. For the eastern Lefkada coastline, the coseismic slips resulted in unremitting subsidence. The respective horizontal coseismic coastal displacements were more profound, consistent with the predominant strike-slip movement. The calculations along with the historical macroseismic effects comprise the basis for both the countermeasures related to coastal preservation and mitigation of the seismic risk from landslides and rock falls that appear in synchronization with the coseismic slip.

**Key words:** strong earthquakes, coastal deformation, Lefkada Island.

### 1. Introduction

Coastal uplift and subsidence are vertical displacements of the crust due to crustal deformation, among other factors, and are broadly and extensively studied along subduction fronts. Coastlines in seismically active areas, are often bounded by certain fault segments that accommodate an appreciable portion of the active deformation and their activity influences the coastal morphology. The coastal evolution is considerably affected by catastrophic earthquakes and their associated tsunamis, in addition to the postglacial sea level rise, with the vertical displacements to be quite localised because of faulting. Emergent coasts are commonly characterised by differential uplift within distinct segments that might be sustained as morphotectonic units on time scales of tens of thousands to millions of years (Melnick *et al.*, 2006). In addition to the vertical displacements, coseismic, earthquake block tilting can be observed from the coast to inland. These observations

have led to a number of studies mainly along tectonically active plate boundary coastlines, aiming to estimate their deformation in areas subject to coseismic movements.

The Lefkada Island belongs to a rapidly deformed area, the central Ionian islands area including the Cephalonia Island as well, dominated by the Cephalonia Transform Fault Zone (KTFZ), stepping the convergence of Apulia and Eurasia to the north and the Hellenic Subduction Zone (HSZ) to the south. The KTFZ comprises major faults that bound the western shorelines or offshore escarpments of both islands and are associated with frequent strong ( $M \geq 6.0$ ) earthquakes. The SKS anisotropy direction found for this area was interpreted by the presence of tearing (Kaviris *et al.*, 2018). The aim of the present study is to assess the effect of the coseismic deformation on the coastal morphology and discuss the related hazards. Sudden coastal uplift and its direct association with earthquakes were first documented by FitzRoy and Darwin in south-central Chile in 1835 (FitzRoy, 1839). Measurements of coseismic coastal uplift and subsidence were systematically started much later and in particular since the 1960s and were investigated in association with the causative fault geometry and faulting style.

Palaeoenvironmental changes of the Lefkada sound were investigated by Brockmuller *et al.* (2007) who reported, in addition to indicators for submergence due to a remarkably rapid rise of the relative sea level, strong tectonic uplift at the northern coastline. The reported indicators evidenced enormous local differences in the tectonic movements. Reconstruction of the palaeoshoreline during the Last Glacial Maximum by Ferentinos *et al.* (2012) displayed that Lefkada Island was separated by a narrow strait from Cephalonia, Ithaca, and Zakynthos, that seemed to relate to each other. Lefkada appeared to relate to the mainland to the east, along with Meganisi and the smaller islands between. During this period the most extended retreat of the sea occurs on the northern and eastern parts of the study area. Field observations carried out by Evelpidou *et al.* (2017) evidenced a total subsidence of  $140 \pm 6$  cm in a period of 1.1 to 5.7 kyr, as deduced from submerged notches mostly along the eastern coastline, and a comparable  $135 \pm 6$  cm during a period lasting between 0.9 and 3.0 kyr, from four submerged fossil shorelines in Meganisi Island. The authors claimed that apart of the similarities, the identified differences indicate that certain coseismic events have a local effect and, in some cases, have affected only part of the study area. Palaeogeographic reconstruction was attempted by Sakellariou *et al.* (2018), who have determined the relative sea level changes in relation to eustatic change, glacio-hydro-isostatic variation, and vertical tectonic movements. The synchronisation of prograding prisms at different depths testify the decisive role of local vertical tectonic movements affecting the evolution of basins and margins during the Late Quaternary, by causing subsidence or uplift of different parts in the study area. These variations were attributed by the authors to vertical tectonic movements along the active faults.

The western coastlines in Lefkada are running parallel to the KTFZ and provide an interesting situation that enables the study of their coseismic deformation and its spatial variance. The eastern part of the island constitutes a coastal wetland occupying the hanging wall of the bounding faults and experienced significant subsidence during the strong events, whereas significant crustal uplift can be found at certain sites along the western coastline. Aiming to investigate the coseismic coastal deformation, firstly an attempt is made to make full exploitation of the historical information for extracting relevant information, and then model the coseismic changes.

In the framework of projects for an in-depth analysis, sea level rise scenarios were created for the Mediterranean region including the coasts of Lefkada city and its adjoining lagoon (Anzidei *et al.*, 2018; Pizzimenti *et al.*, 2018). During this investigation a high-resolution 3D mapping

of the area was realised (Patias *et al.*, 2018) resulting in producing a digital surface model and an orthophoto of the study area with a resolution of 4 and 2 cm, respectively. Furthermore, the integration of the high resolution topographic data was integrated with the expected sea level rise from IPCC AR5 2.6 and 8.5 climatic scenarios to map sea level rise scenarios for 2050 and 2100, taking into account the vertical land motion as estimated from CGPS data. As a result, coastal coseismic subsidence or uplift can be used to enhance the developed models for the estimation of coastal flooding. Seismicity monitoring is a powerful tool for even the identification of shipwreck characteristics (Fiaschi *et al.*, 2017), whereas coseismic displacements in the study area were extensively studied with geodetic measurements (e.g. Sakkas and Lagios, 2017; Ganas *et al.*, 2018; among others).

Here the mode of coseismic deformation is mainly caused by dextral strike-slip movements along with a significant thrust component, attributed to the coastline elevation changes induced by the strong earthquake occurrence. The target is to constrain the elevations of uplift and subsidence of the shorelines and the results of this investigation allow to assess the coastal changes. Emerged shorelines have been long used as geomorphic markers for estimating the permanent surface deformation and inferring the kinematics and slip rate of local faults. Studying the relation between the motion of these structures during strong earthquakes may contribute to seismic hazard assessments and our understanding of the build-up of topography.

## 2. Seismotectonic setting

The Lefkada Island is part of the central Ionian seismic zone, dominated by the rapid deformation of the KTFZ that bounds this zone from the west. The KTFZ consists of an active boundary between the continental collision of Adriatic microplate and Eurasia to its north, and the subduction of the east Mediterranean oceanic crust beneath the Aegean microplate to its south. The dextral strike-slip nature of the KTFZ was firstly introduced by Scordilis *et al.* (1985), who determined the fault plane solution of the 1983 Cephalonia  $M=7.0$  earthquake, and then confirmed by waveform modelling (Kiritzi and Langston, 1991; Papadimitriou, 1993). The dextral strike-slip sense of motion is documented by the fault plane solution of the 2003 Lefkada  $M=6.2$  main shock, the 2014 Cephalonia doublet ( $M=6.1$  and  $6.0$ ) and the 2015 Lefkada  $M=6.5$  main shock, all associated with fault segments comprised in the KTFZ.

The two major KTFZ segment boundaries, namely the Lefkada and Cephalonia segments, present abrupt morphologic characteristics along the western shorelines of both islands (Fig. 1) and differ slightly in strike and maximum observed earthquake magnitude ( $M_{max}=7.4$  for Cephalonia and  $M_{max}=6.7$  for Lefkada, from historical records that are rather slightly exaggerated). The seismicity is mainly aligned along strike of the boundaries, producing frequent strong earthquakes, separated by periods of low seismicity evidencing possible triggering through stress transfer between the fault segments (Papadimitriou, 2002). The seismogenic layer is shallow and reaches a depth that does not exceed the 20 km, as verified by the highly accurate relocated recent seismicity. The seismicity forms a relatively narrow band and appears more sparse as one goes onshore, while is almost totally lacking at the eastern coasts and the offshore area, to the east of both islands. Seismic activity related to faults of different orientation is also present.

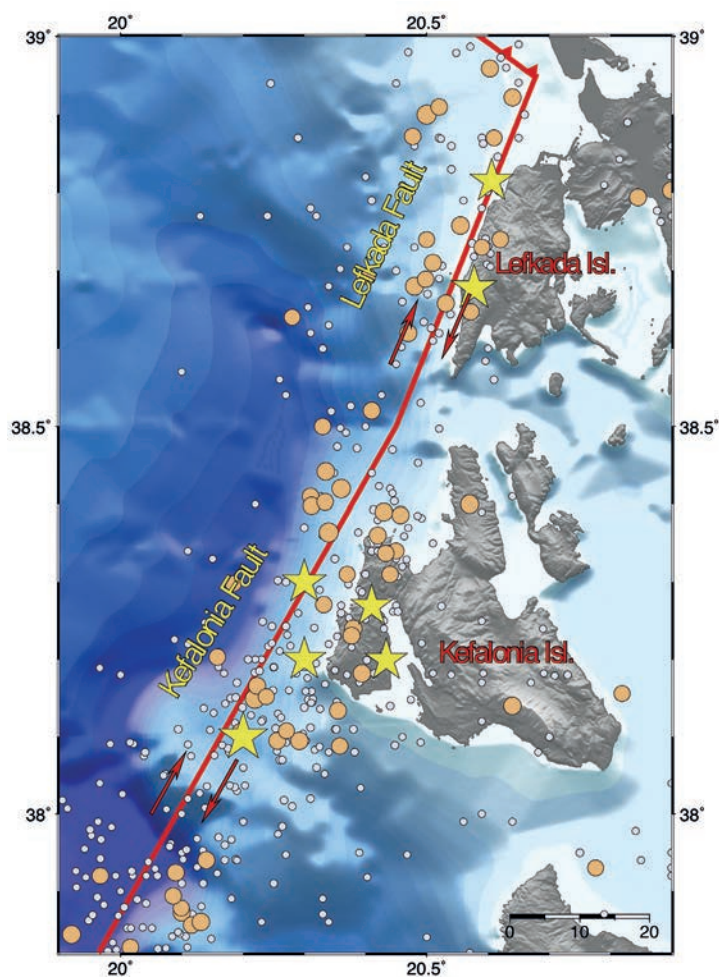


Fig. 1 - Morphology, major faults and seismicity since 1970 in Lefkada and Cephalonia islands. Stars depict the  $M \geq 6.0$  earthquakes, bigger circles the  $5.9 \geq M \geq 5.0$  and smaller circles the  $4.9 \geq M \geq 4.5$  ones.

### 3. Seismic activity

In an attempt to provide a comprehensive view of historical and instrumental seismicity in the study area, the main characteristics of the historical records and the relocated seismicity are engaged. The majority of larger and smaller magnitude instrumental seismicity is located slightly offshore and onshore close to the shoreline. The macroseismic descriptions for the most damaging historical earthquakes are in accordance and emphasize the locus of strong shakings.

#### 3.1. Strong historical earthquake occurrence

Information on the historical seismicity in the study area starts in 1577, and in evidently regular basis and continuously since the beginning of the 17th century. This information is reported in Table 1, where from it appears that during the past five centuries strong ( $M \geq 6.0$ ) earthquakes with recurrence intervals of 30-50 years occurred in the study area, showing a strong clustering (Fig. 2). Magnitudes in the early historical catalogue exhibit an upper limit of 6.7, which has

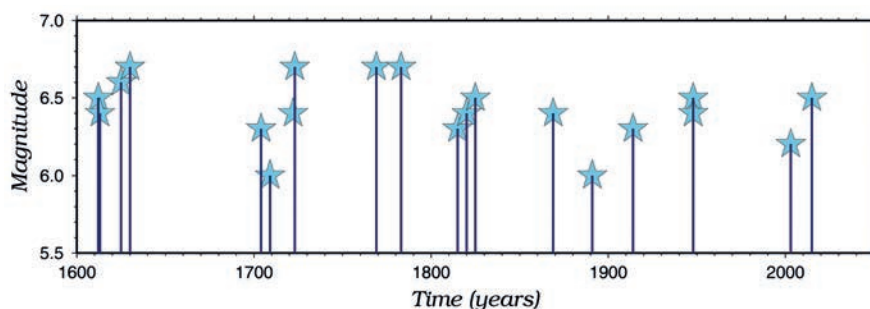


Fig. 2 - Temporal distribution of strong ( $M \geq 6.0$ ) known historical earthquake activity in Lefkada island.

been repeatedly reached in the 17th and 18th century, although never afterwards. We may, then, speculate about an overestimation in magnitude at that time and that the maximum observed,  $M_{obs}$ , and expected,  $M_{max}$ , magnitudes equals to 6.5.

There is evidence of localised coseismic deformation after the occurrence of strong events in the study area, that was shaken almost every 30-40 years. A series of maps showing the positions of the reported damage (Papazachos and Papazachou, 2003) is shown in Fig. 3 and in some cases calculated intensities. From the macroseismic descriptions and instrumental locations, it is derived that two discrete fault segments bounding the west coastline are responsible for this strong activity, which appeared to fail consecutively several times. For hazard assessment, it is

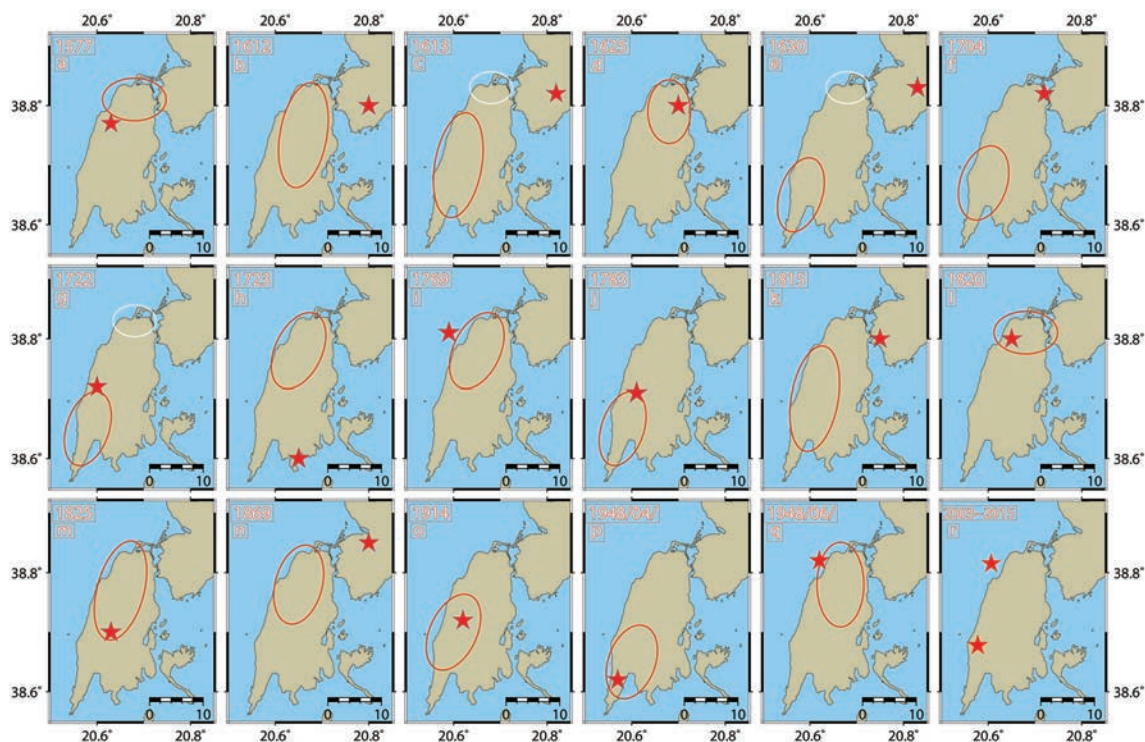


Fig. 3 - Epicentral distribution of known strong ( $M \geq 6.0$ ) earthquakes since 1500 depicted by the red stars. Red ellipses comprise the devastated areas and the white ones only in the cases where minor damage was reported for the city of Lefkada (located in the northern coast).

important to determine whether the earthquake occurred on the North Lefkada fault, the South Lefkada fault, or another fault in the area.

Reports describing earthquake destructions in Lefkada city are more numerous than the ones referred to other parts of the island or the small villages. In fact, the only important urban area is at this location during its complete historic period. Given that the quantity and quality of the felt reports depend upon the development of the local cities, this is the reason why the earthquakes in the early historical archives are referred to the island’s capital. This is exactly the case of the first reported earthquake in 1577, with  $M=6.2$  and its macroseismic epicentre near the area of maximum reported damage (Fig. 3a).

A cluster of four ( $6.4 \leq M \leq 6.7$ ) earthquakes took place between 1612-1630. Extensive damage throughout the island was reported for the 1612  $M=6.4$  earthquake, the macroseismic epicentre of which was put onshore the Greek mainland (Fig. 3b). The collective information would support the North Lefkada fault segment failure. This comes in line with the next occurrence in the next year with an  $M=6.5$  in 1613 for which the associated damage is mostly in the south-western part, implying failure of the South Lefkada fault segment, although its epicentre is again put onshore the Greek mainland (Fig. 3c). The effects of the 1625 and 1630 shocks are considerably localised

Table 1 - Macroseismic effects of the known historical earthquakes ( $M \geq 6.0$ ) at specific sites of Lefkada Island (after Papazachos and Papazachou, 2003).

|       | City of Lefkada | East coastline | Western coastlines | Northern part | Central part | Southern part |
|-------|-----------------|----------------|--------------------|---------------|--------------|---------------|
| 1577  | ■               |                |                    |               |              |               |
| 1612  | *               |                |                    | *             | *            |               |
| 1613  | ☆               |                |                    | ☆             | ☆            |               |
| 1625  | ■               | ■              |                    |               |              |               |
| 1630  |                 |                |                    |               | ■            | ■             |
| 1704  |                 |                |                    |               | ■            | ■             |
| 1722  | ❖               |                |                    |               | ■ ☆          | ■ ☆           |
| 1723  | ☆               | ≈              |                    | ☆             |              |               |
| 1769  | ■ ☆             | ■              |                    |               |              |               |
| 1783  |                 |                | ■                  |               | ■            |               |
| 1815  | *               |                |                    | *             | *            | *             |
| 1820  | ■               | #              |                    |               |              |               |
| 1825  |                 |                |                    | ■             |              |               |
| 1869  |                 | ≈              |                    | ■             |              |               |
| 1914  | ❖               | ≈ #            | ■                  |               | ■            | ❖             |
| 1948A |                 |                | ■                  |               | ■            | ■ ≈           |
| 1948B |                 | #              |                    | □             |              |               |
| 2003  |                 |                |                    | □             |              |               |
| 2015  |                 |                |                    |               | □            | □             |

Notation: ■ localised damage, \* disperse damage, ☆ building collapse, □ rockfalls and landslides, # flooding and subsidence, ≈ tsunami indication, ❖ slight damage reported.

in comparison with the previous descriptions, indicating ruptures of the north and south fault segments, respectively (Figs. 3d and 3e).

After more than 70 years of paucity in strong earthquakes occurrence, the southern part was shaken in 1704 (Fig. 3f) and then, close in time, in 1722 and 1723 in the southern (Fig. 3g) and, then, in the northern part (Fig. 3h), respectively, although the epicentre of the latter is given at the southern onshore area. In less than 50 years of quiescence, the next seismic excitation started in 1769 taking place at the northern segment (Fig. 3i) and in a few years across the southern segment (Fig. 3g). After a shorter quiescent period of about 30 years, a triplet has shaken the island, with extensive reported damage in 1815, in the southern and central western part (Fig. 3k), more localised near the city of Lefkada in 1820 (Fig. 3l), and the northern part in 1825 (Fig. 3m). The proximity of the damaged areas that were attributed to  $M \geq 6.0$  earthquakes, makes doubtful the location of consecutive failures at the same fault segment. This is a point for further investigation with accurate locations to identify the fault network and possible smaller faults, but capable to produce severe damage and constitute a threat to the city of Lefkada, at the same degree as the major faults. After 44 years the northern segment again failed in 1869 (Fig. 3n), and after 45 years the southern segment in 1914 (Fig. 3o). A doublet interrupted the 34 years quiescence, in 1948 when the western part of the island was considerably devastated in a time span of 2 months (Figs. 3p and 3q). A longer quiescent period of 53 years paused by the 2003 main shock associated with a fault running parallel to the north-western coastline (Karakostas *et al.*, 2004) and then in 2015, the southern coastline bounding fault failed (Papadimitriou *et al.*, 2017), to accomplish one more seismic cycle of the Lefkada major faults system (Fig. 3r).

### 3.2. Recent activity and seismic sequences

Offshore seismicity was poorly constrained before 2003 because of the sparsity of the seismological network, with all but one (in south Cephalonia Island) stations being located onshore in the Greek mainland and far from the KTFZ. The installation of a comparatively dense temporary seismological network in 2003, one day after the main shock occurrence, enabled the recording of hundreds of aftershocks and their relocation with greatly improved accuracy (Karakostas *et al.*, 2004). The aftershock seismicity, which was extended far beyond both edges of the main rupture, was for the first time found to be positioned partly onshore, instead of far offshore as it was previously considered (white circles in Fig. 4). Extensive landslides and rockfalls accompanied the occurrence of the main shock, mainly along the coastal slopes. The installation and continuous operation of permanent seismological stations since 2007 resulted to the accurate locations that revealed details on the secondary faults activated along the main rupture (Karakostas and Papadimitriou, 2010) and on the faulting network along the KTFZ (Karakostas *et al.*, 2010), which were also verified by geodetic data and analysis (Ilieva *et al.*, 2016).

The closely installed seismological stations provided valuable data at the time of the second seismic excitation in 2014, with two main shocks of  $M=6.1$  and  $M=6.0$  that occurred on 26 January and 3 February, respectively. Most importantly, it happened that in the 2015 Lefkada seismic excitation, very close to the main rupture (much less than 5 km) closely spaced stations surrounded the activated area and provided data, where from P and S arrivals were again manually picked and by the use of the double-difference (DD) hypoDD (Waldhauser and Ellsworth, 2000; Waldhauser, 2001) the location accuracy was again improved. It is now more onshore shifted (green circles in Fig. 4) than the 2003 seismicity, concentrated along the Paliki

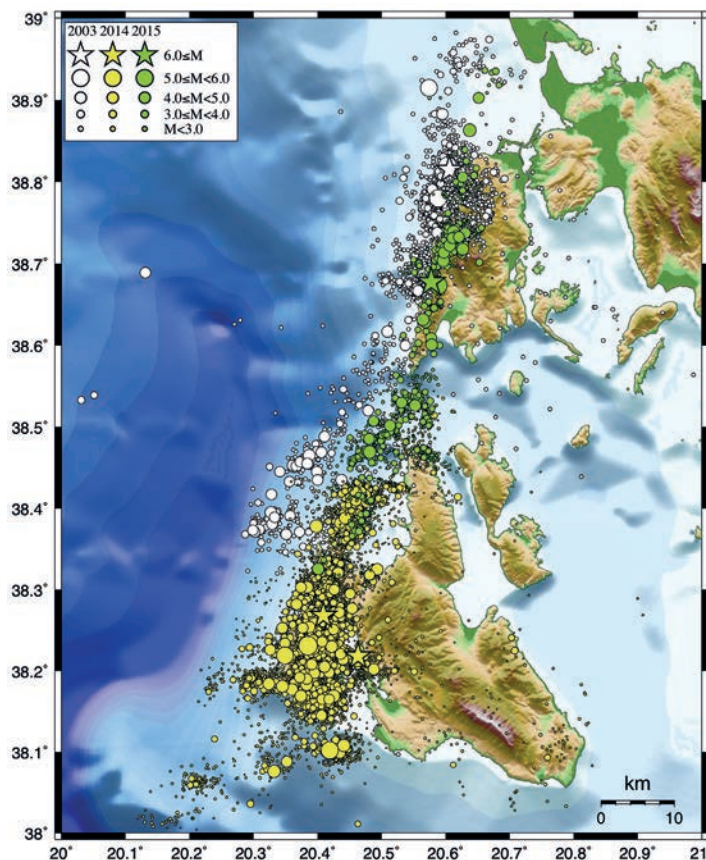


Fig. 4 - Locations of aftershock epicenters in the three more recent seismic sequences (2003 white coloured, 2014 coloured in yellow and 2015 in green). Stars depict the mainshock epicenters. The shift from offshore to onshore location as a function of time and consequently location improvement, is evidenced.

Peninsula in the western part of Cephalonia Island, along with the off-fault aftershocks. In all three seismic excitations multi-fault activation was verified, probably triggered by the Coulomb stress changes caused by the main shock slip (Karakostas *et al.*, 2004, 2015; Papadimitriou *et al.*, 2017). The relocated seismicity is mainly concentrated along the fault segments comprised in the KTFZ. Even the background seismicity is considerably lower elsewhere, as one goes far from the KTFZ.

#### 4. Coastal movements from coseismic displacements

In Lefkada Island, the geomorphological evidence, such as cliffs along the western shoreline, indicates that the western coasts have been uplifting steadily, whereas the existence of wetlands and low elevation of the eastern coasts show that this area has been continuously subsiding. Historical descriptions lead to the identification of elongated zones of reported damage and their orientation parallel to the western shoreline. These descriptions support a model in which coseismic uplift produced by the along coast earthquakes and is responsible for the



present coastal landscape characterized by cliffs and rocky promontories, alternating with sand filled beaches. Strain energy that is accumulated in the interseismic stage is released during an earthquake, and the resulted stress changes induce crustal deformation. It is in general difficult to discriminate between the coseismic from the post and interseismic components, the interseismic one might be in some cases of most importance in tectonic uplift and evolution of the coast. The interseismic deformation, nevertheless, is slow, typically in the order of a few mm/yr, whereas the coseismic deformation occurs within a very short time and its maximum values can reach several metres.

Aiming to investigate the impact of recent strong earthquakes that occurred along the KTFZ on the Lefkada coastlines deformation, the displacements caused by these events are calculated by putting coseismic displacements on ruptured fault segments. A dislocation model of a planar surface,  $\Sigma$ , embedded in a homogeneous semi-infinite elastic medium, i.e. a half-space with zero traction on the Earth's surface. Steketee (1958) showed that the displacement field  $u_k$  ( $k$ -th component of  $u$ ) in a semi-infinite elastic medium for an arbitrary uniform dislocation,  $U$ , across a surface,  $\Sigma$ , can be determined from

$$u_k = \frac{U_i}{8\pi\mu} \iint_{\Sigma} w_{ij}^k v_j d\Sigma \quad (1)$$

where  $\mu$  is the shear modulus,  $v_j$  are the direction cosines of the normal to the dislocation surface,  $U_i$  is the  $i$ -th component of  $U$ , and  $W_{ij}^k$  are six sets of Green's functions.

For the calculation of the coastal movements caused by the recent strong earthquakes in Lefkada coastlines, the rupture models are approximated with rectangles embedded in the Earth's brittle crustal layer. Fault surfaces are defined by their geometrical parameters, their length,  $L$ , and width,  $w$ , and the parameters provided by the fault plane solutions. The coseismic slips show dominantly right-lateral strike-slip motions, therefore, the dominant coseismic movement is expected to appear in the horizontal components of deformation. The dimensions of the coseismic ruptures are well constrained by aftershock relocation and elaboration of their 3D distribution [after Karakostas *et al.* (2004) for the 2003 Lefkada main shock; Karakostas *et al.* (2014, 2015) for the 2014 doublet that occurred in Cephalonia Island; Papadimitriou *et al.* (2017) for the 2015 Lefkada main shock]. The values of the scalar moment for each earthquake were adopted from the global centroid moment solutions (<http://www.ldeo.columbia.edu/~gcmt/>) and the GFZ moment tensor solution (<https://geofon.gfz-potsdam.de/eqinfo/event.php?id=gfz2014cinv>) and an average slip was calculated from these values and fault dimensions (Table 2) considering rigidity equal to  $3.3 \times 10^5$  bar.

The 2003 main shock faulting parameters were taken from the global centroid moment tensor (gcmt) solution, as they agree with the aftershock analysis (Karakostas *et al.*, 2004). For the 2014 doublet, the geometry of the southern cluster was considered to represent the main rupture, since it was activated in the first day of the seismic excitation, whereas the cluster at the northernmost part of the Paliki Peninsula the second main shock rupture area (Karakostas *et al.*, 2014, 2015). The GFZ moment tensor solution agrees very well with the geometry of the second main shock aftershock zone. As the dip and the sense of slip of the 26 January shock are the same as the 3 February one, a similar value for the rake was used. For the 2015 main shock the gcmt solution was used with a slight modification for the strike ( $16^\circ$  instead of  $22^\circ$ ) considering the trend of the aftershock zone (Papadimitriou *et al.*, 2017).

Table 2 - Rupture models for the earthquakes included in the displacements calculation model.

| DATE          | TIME     | Latitude ( $\phi^\circ$ N) | Longitude ( $\lambda^\circ$ E) | L (km) | u (m) | $M_w$ | Mechanism |     |      |
|---------------|----------|----------------------------|--------------------------------|--------|-------|-------|-----------|-----|------|
|               |          |                            |                                |        |       |       | Strike    | Dip | Rake |
| 2003, Aug. 14 | 05:14:55 | 38.815                     | 20.606                         | 16     | 0.60  | 6.2   | 18        | 60  | -175 |
| 2014, Jan. 26 | 13:55:41 | 38.199                     | 20.434                         | 13     | 0.38  | 6.1   | 20        | 65  | 177  |
| 2014, Feb. 03 | 03:08:44 | 38.269                     | 20.410                         | 11     | 0.52  | 6.0   | 12        | 57  | 157  |
| 2015, Nov. 17 | 07:10:07 | 38.6775                    | 20.5773                        | 17     | 1.43  | 6.5   | 16        | 64  | 179  |

#### 4.1. Vertical coastal coseismic displacements

Fig. 5 shows the vertical coseismic displacements caused by the four mainshocks. The maps comprise both islands for the sake of comparison and extent of influence in coastal deformation. The vertical deformation reached 5 cm of uplift at the central western Lefkada shoreline, just beyond the 2003 rupture fault tip, consistent with the expected deformation from the reverse component of the dominantly strike-slip faulting in an elastic half-space (Okada, 1985). The area where the vertical displacement exceeded 2 cm extends along the coastlines of southern Lefkada and north-western Cephalonia Islands (Fig. 5a). Significant subsidence is estimated for the northern Lefkada shorelines and in particular in the city of Lefkada, where considerable damage was reported for the harbour and the buildings, with one of them being collapsed. Landslides and rockfalls were mainly observed along the NW part of the island, almost delineating the main rupture area, where subsidence was estimated (blue dots in Fig. 5a). The magnitude of the vertical displacement is of much less importance in Cephalonia Island, without reported damage. The 2014 Cephalonia doublet resulted in slight subsidence of the Lefkada’s western shoreline (Figs. 5b and 5c).

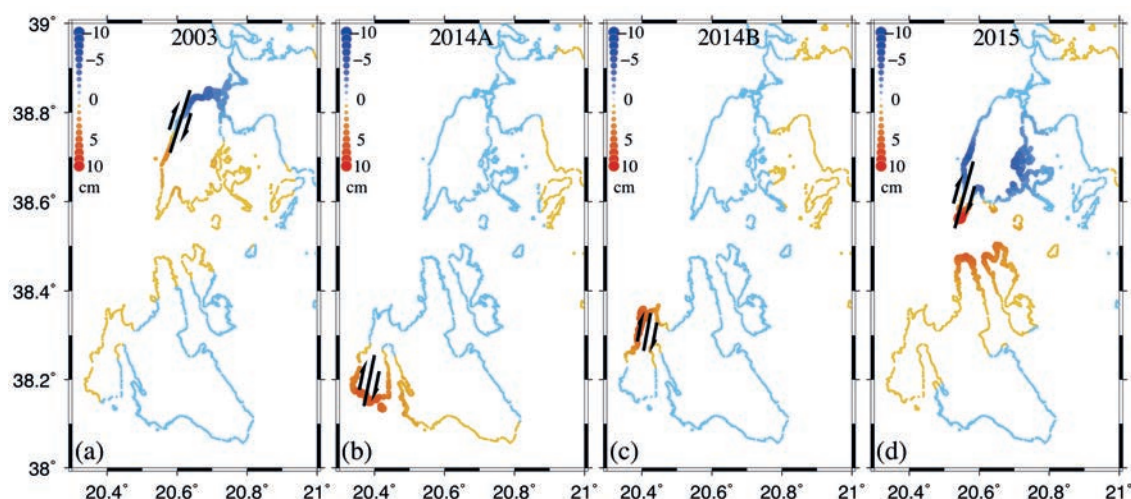


Fig. 5 - Coastal coseismic vertical deformation due to the occurrence of the main shocks that occurred in 2003 in Lefkada (a), in January 2014 in southern Paliki Peninsula (b), in February 2014 in northern Paliki Peninsula (c) and in 2015 in southern Lefkada Island (d). Circles denote calculation points, sized and coloured by their amounts of uplift (blue denotes subsidence).

For the 2015 Lefkada main shock that occurred to the south of the 2003 one, the more significant subsidence (up to 8 cm) was estimated for the central western coast, close to the villages with the most devastating effects (Fig. 5d). At the same sites and the small south bay, coastline road cracks were observed (Ganas *et al.*, 2016; Kassaras *et al.*, 2018) in addition to slope failures that were more extensively distributed on the island. Details on the static deformation given by Avalone *et al.* (2017) report a subsidence related with the 2015 main shock of  $\sim 4.3 \pm 1.2$  cm at a particular site, which is slightly smaller than our modelled values, and uplift of  $\sim 7.5$  cm to its SE, slightly larger than ours, and subsidence of  $\sim 11.0$  cm to its SW, which does not agree with our calculations.

Two displacement boundaries are recognized in each case, between uplift and subsidence, with the discontinuity lines to be located in both islands, independently of the deformation size. As shown in Fig. 4, we can recognize significant vertical displacements for each one of the islands where the causative faults are located.

#### 4.2. Horizontal coastal coseismic displacements

The prevailing strike-slip faulting led us to examine the degree of the influence from the horizontal coseismic displacements. As in the previous figure, the displacements are given on discrete points along the coastlines and are computed for each one of the main shocks listed in Table 2 and are plotted in Fig. 6. The sense of motion and its size at each point are represented by the vector azimuth and length, according to the scale given on the top of the subfigures. As expected from the elastic dislocation model the horizontal displacements are much larger in values than the vertical ones. It is worth noting that the entire coastline of Lefkada Island has been undergone coseismic horizontal displacements of several centimetres, during both 2003 and 2015 main shocks (Figs. 6a and 6d). A considerable movement has incurred in the coastlines of the nearby mainland, as well as the northern coastlines of Cephalonia and Ithaca islands. The 2014 Cephalonia doublet, on the other hand, did not seriously affect the Lefkada coastlines (Figs. 6b and 6c).

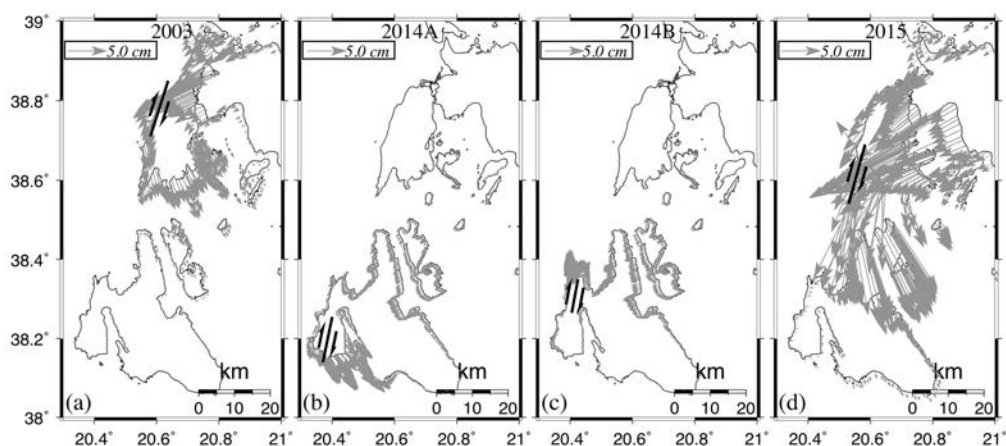


Fig. 6 - Coastal horizontal static displacements, with arrows lengths according to the scale given at the upper left side of each figure. Surface fault projections along with the sense of coseismic slip is given in each case: a) for the 2003 main shock with  $M=6.2$  that occurred along the NW Lefkada coastline; b) for the 26 January 2014 main shock with  $M=6.1$  that occurred in the southern Paliki Peninsula, in Cephalonia Island; c) for the 3 February 2014 main shock with  $M=6.0$  that occurred in the northern Paliki Peninsula, in Cephalonia Island; d) for the 2015 main shock with  $M=6.5$  that occurred along the SW Lefkada coastline.

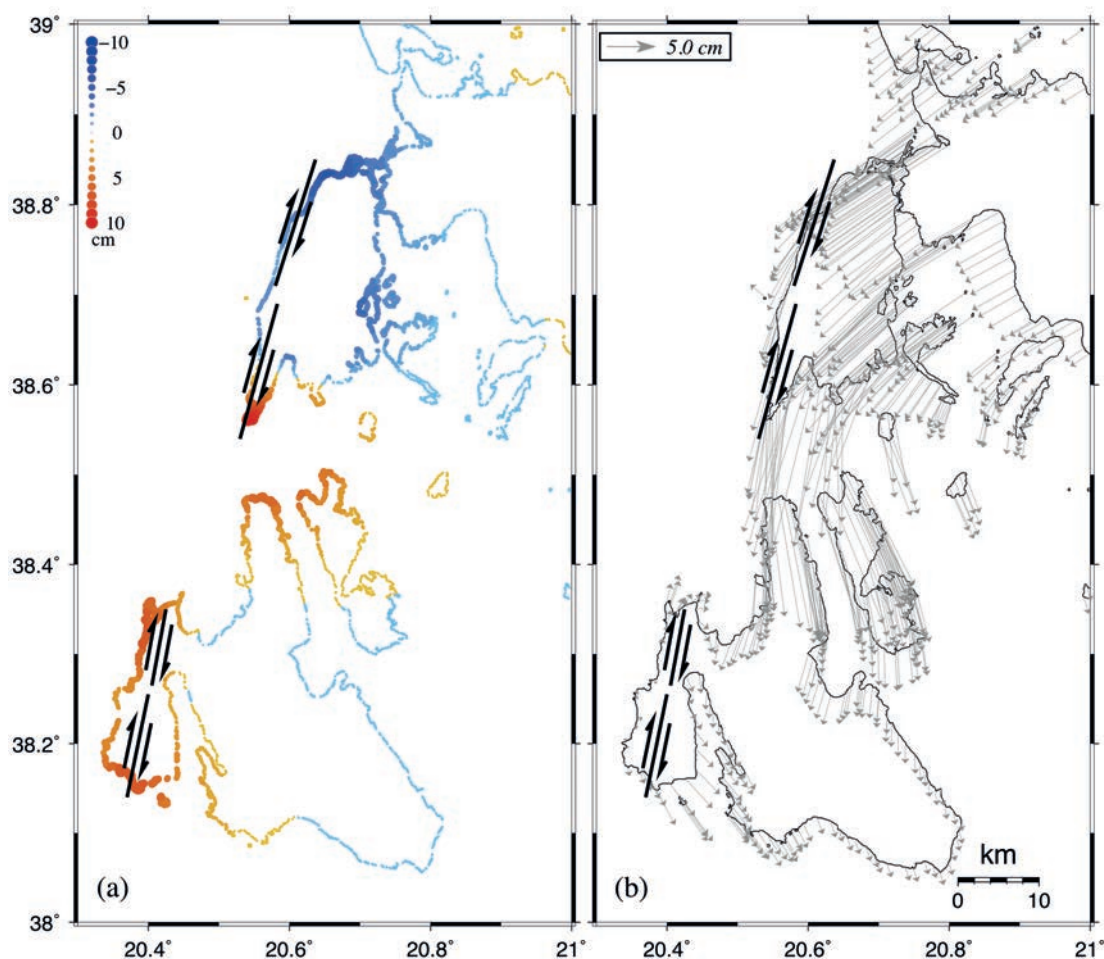


Fig. 7 - Cumulative coastal vertical and horizontal static displacements. Symbols are as in Figs. 5 and 6.

#### 4.3. Cumulative coastal coseismic displacements

The cumulative results in both vertical and horizontal coseismic displacements are shown in Fig. 7. It appears that the southern edge of Lefkada coastlines undergoes uplift, by strong events that occurred on fault segments of the KTFZ, while along the northern coastline a continuous subsidence occurs (Fig. 7a). The cumulative horizontal movements are consistent with a counterclockwise rotation of the central Ionian islands area (Fig. 7b), with more intense movement being observed in Lefkada.

#### 4.4. Profiling the vertical coastal coseismic displacements

We determined the amount of coseismic crustal deformation, approximately parallel to the main ruptures strike at close positioned points that mark the western Lefkada coastlines (Fig. 8). The along coast profiles attest the periodic coseismic uplift and subsidence, depending upon the location of the rupture plane. The maximum uplift of approximately 10 cm was estimated at the southern edge of the coast, caused by the 2015 rupture and by 4 cm in 2003 main shock. The amount of uplift rapidly decreases by about the same value up to the maximum subsidence, reaching high negative values. In 2003 case further to the south, the uplift was diminished up to

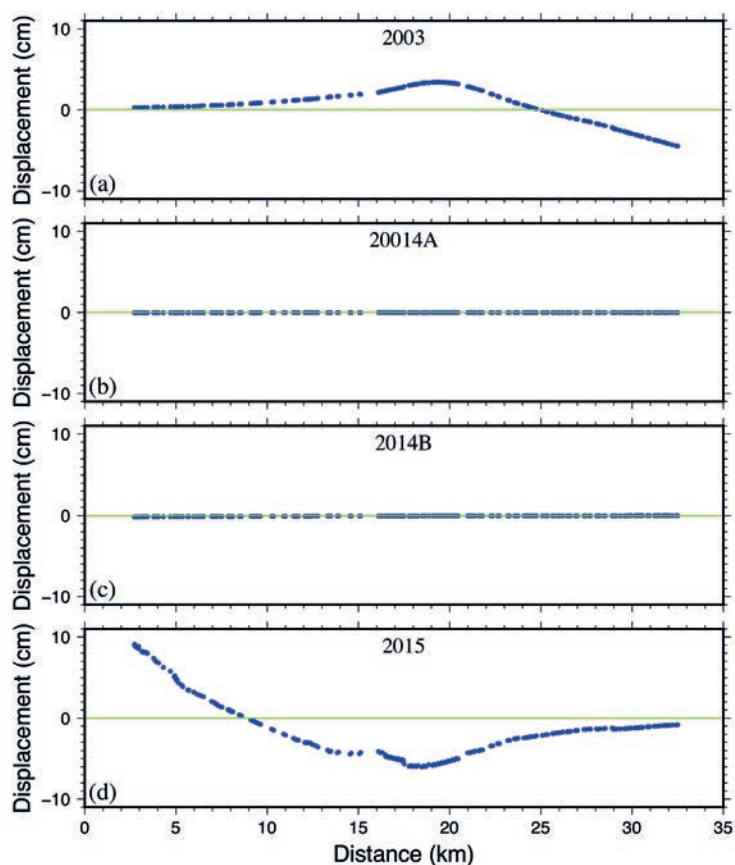


Fig. 8 - Vertical displacement along the western Lefkada Island shoreline due to the coseismic slip of the four main shocks: a) 14 August 2003, b) 26 January 2014, c) 3 February 2014, and d) 17 November 2015, main shocks, respectively.

almost zero, whereas to the north minor subsidence took place up to the north coastal edge (Fig. 8a). During the 2015 rupture rapid alteration of uplift and subsidence appeared along the south and central coastline, and gradually increases to almost zero at the northern edge (Fig. 8d). Both 2014 Cephalonia events resulted in almost zero vertical motion along the entire coastline (Figs. 8b and 8c). Summing up the coseismic coastal deformation, it is evident that the southern part of western Lefkada is seismically steadily uplifted, whereas the maximum subsidence takes place at the northernmost part (Fig. 9).

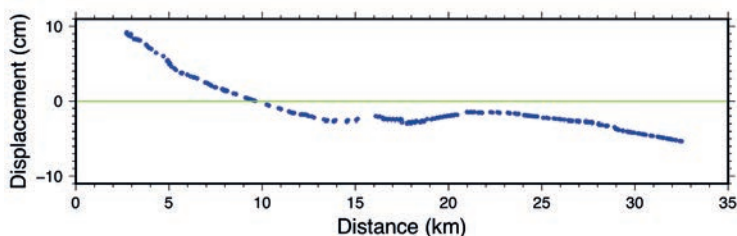


Fig. 9 - Cumulative vertical displacement along the western Lefkada Island shoreline due to the coseismic slip of the four main shocks.

## 5. Discussion and conclusions

Quantitative estimations for the expected casualties of future strong earthquakes, which constitute an indispensable component for realistic countermeasures and seismic risk mitigation, are thought to be based on modelling the deformation associated with the coseismic slip of past earthquakes. In this study, we “integrated” the macroseismic descriptions of the earthquakes that occurred since the 16th century in Lefkada Island and considered that earthquakes should repeat with similar locations and magnitudes. The source areas of the historical events are traced according to the available published descriptions in Papazachos and Papazachou (2003), and in parallel they were correlated and found in accordance with the rupture areas of the instrumental earthquakes.

Estimating the deformation caused by the coseismic slip of strong earthquakes in an area, and in particular, at the sites where strong historic earthquakes have happened, provides the means to evaluate the extent of the influence in the coastal topography. We surveyed the extent and magnitude of the observed coastal changes reported in historical records that could be directly compared with the contemporaneous estimations, and the results are devoted to being used for mitigating the impact of future earthquake damage.

To give an estimation of the future hazard and the frequency of the main shock occurrence, a rough estimation of their recurrence is made by taking into account the major faults slip rate. If the South Lefkada fault segment has a horizontal slip rate of  $\sim 15$  mm/yr, it accumulates  $4.95 \times 10^{11}$  dyn $\times$ cm of moment per year per  $\text{cm}^2$  of fault area, using a shear modulus of 33 GPa. The total area of the causative fault is approximately  $2 \times 10^{12}$   $\text{cm}^2$  (Papadimitriou *et al.*, 2017). Using this area and annual rate, it takes roughly 71.5 years to accumulate the amount of the moment release in the 2015 earthquake, which equals to  $7.15 \times 10^{25}$  dyn $\times$ cm. This estimate overpasses the time of 67 years that have elapsed since the most recent strong main shock along this fault segment (1948) and implies that the strain accumulated at the fault area since the last event, has been completely relaxed. From a Coulomb stress transfer perspective, in which slip on a given fault triggers motion on the adjacent segment, contributing to unclamping of the seismogenic part of the second fault, the failure of the 2015 segment could be expected earlier. The presence of positive Coulomb - stress changes imposed by the 2003 main shock onto the 2015 fault, argues that over a short time scale, both major fault segments may fail, and this became more obvious from the doublet in 1948 taking place over a short time scale of only 2 months. Both recent main shocks in 2003 and 2015 caused surface deformation that was broadly distributed, uplift in localised areas along the western Lefkada shoreline and regularly clear subsidence in areas of the eastern shoreline, implying that the coseismic slip of this type of events that are the “characteristic” ones in the area, contribute to the current coastal morphology.

Our estimations and assessments can then be summarised in the following:

1. coastal uplift and subsidence of several cm takes place coseismically with the stronger ( $M \geq 6.0$ ) main shocks;
2. the strong main shocks that occur in Cephalonia Island have subtle influence on the coastal deformation in Lefkada;
3. given that the major faults are located or bound the western Lefkada shoreline, the city of Lefkada undergoes continuous coseismic subsidence.

**Acknowledgements.** The editorial assistance of Alessandro Vuan along with the constructive comments of Athanassios Ganas are greatly appreciated. Fault plane solutions data used in this paper came from <http://www.ideo.columbia.edu/~gcmt/>. Part of this work was funded by the European research project SAVEMEDCOASTS (Sea level rise scenarios along the Mediterranean coasts GA No. ECHO/SUB/2016/742473/PREV16). SAVEMEDCOASTS is a cooperation European project co-funded by the ECHO European Commission Unit (EU Humanitarian Aid and Civil Protection) and published sources listed in the references. The stress tensors were calculated using a program written by J. Deng (Deng and Sykes, 1997), based on the DIS3D code of S. Dunbar, which later improved (Erikson, 1986) and the expressions of G. Converse. The plots were made using the Generic Mapping Tools version 5.4.4 (Wessel *et al.*, 2013). Part of this work was funded by the European research project SAVEMEDCOASTS (Sea level rise scenarios along the Mediterranean coasts GA No. ECHO/SUB/2016/742473/PREV16). SAVEMEDCOASTS is a cooperation European project co-funded by the ECHO European Commission Unit (EU Humanitarian Aid and Civil Protection). Geophysics Department Contribution 918.

## REFERENCES

- Anzidei M., Patias P., Georgiadis Ch., Doumaz F., Kaimaris D., Pikridas Ch., Brunori C.A., Loizidou X., Michetti M., Petsa D., Orthodoxou D., Torresan S., Furlan E., Trivigno M.L., Greco M., Serpelloni E., Vecchio A. and Pizzimenti L.; 2018: *Expected sea level rise scenarios by 2100 along targeted coasts of the Mediterranean: new results from the SAVEMEDCOASTS project*. In: Proc. 20<sup>th</sup> EGU General Assembly, Vienna, Austria, p. 9003.
- Avalone A., Cirella A., Cheloni D., Tolomei C., Theodoulidis N., Piatanesi A., Briole P. and Ganas A.; 2017: *Near-source high-rate GPS, strong motion and InSAR observations to image the 2015 Lefkada (Greece) earthquake rupture history*. Sci. Rep., **7**, 10358, doi: 10.1038/s41598-017-10431-w.
- Brockmuller S., Vott A., May S.M. and Bruckner H.; 2007: *Palaeoenvironmental changes of the Lefkada sound (NW Greece) and their archaeological relevance*. Coastline Rep., **9**, 127-138.
- Deng J. and Sykes L.; 1997: *Evolution of the stress field in Southern California and triggering of moderate size earthquakes: a 200-year perspective*. J. Geophys. Res., **102**, 9859-9886.
- Erickson L.; 1986: *User's manual for DIS3D: a three-dimensional dislocation program with applications to faulting in the Earth*. Master's Thesis, Stanford Univ., Stanford, CA, USA, 167 pp.
- Evelpidou N., Karkani A. and Pirazzoli P.; 2017: *Late Holocene tectonic implications deduced from tidal notches in Leukas and Meganisi Islands (Ionian Sea)*. Geol. Acta, **15**, 1-9, doi: 10.1344/GeologicaActa2017.15.1.1.
- Ferentinos G., Gkioni M., Geraga M. and Papatheodorou G.; 2012: *Early seafaring activity in the southern Ionian Islands, Mediterranean Sea*. J. Archaeol. Sci., **39**, 2167-2176, doi: 10.1016/j.jas.2012.01.032.
- Fiaschi A., Matassoni L., Lotti A. and Saccorotti G.; 2017: *Micro-seismic monitoring after the shipwreck of the Costa Concordia at Giglio Island (Italy)*. Acta Geophys., **65**, 1019-1027.
- FitzRoy R.; 1839: *Narrative of the surveying voyages of His Majesty's Ships Adventure and Beagle between the years 1826 and 1836, describing their examination of the southern shores of South America, and the Beagle's circumnavigation of the globe*. Proceedings of the second expedition, 1831-36, under the command of Captain Robert Fitz-Roy, R.N., Henry Colburn, London, U.K., vol. II, 698 pp.
- Ganas A., Elias P., Bozionelos G., Papathanassiou G., Avallone A., Papastergios A., Valkaniotis S., Parcharidis I. and Briole P.; 2016: *Coseismic deformation, field observations and seismic fault of the 17 November 2015  $M_w$  6.5, Lefkada Island, Greece earthquake*. Tectonophysics., **687**, 210-222.
- Ganas A., Andritsou N., Kosma C., Argyrakis P., Tsironi V. and Drakatos G.; 2018: *A 20-yr database (1997-2017) of co-seismic displacements from GPS recordings in the Aegean area and their scaling with  $M_w$  and hypocentral distance*. Bull. Geol. Soc. Greece, **52**, 98-130, doi: 10.12681/bgsg.18070.
- Ilieva M., Briole P., Ganas A., Dimitrov D., Elias P., Mouratidis A. and Charara R.; 2016: *Fault plane modeling of the 2003 August 14 Lefkada Island (Greece) earthquake based on the analysis of ENVISAT SAR interferograms*. Tectonophysics., **693**, 47-65, doi: 10.1016/j.tecto.2016.10.021.
- Karakostas V.G. and Papadimitriou E.E.; 2010: *Fault complexity associated with the 14 August 2003  $M_w$  6.2 Lefkada, Greece, aftershock sequence*. Acta Geophys., **58**, 838-854, doi: 10.2478/s11600-010-0009-6.
- Karakostas V.G., Papadimitriou E.E. and Papazachos C.B.; 2004: *Properties of the 2003 Lefkada, Ionian Islands, Greece, earthquake seismic sequence and seismicity triggering*. Bull. Seismol. Soc. Am., **94**, 1976-1981.
- Karakostas V.G., Papadimitriou E.E., Karamanos Ch.K. and Kementzetzidou D.A.; 2010: *Microseismicity and seismotectonic properties of the Lefkada-Cephalonia seismic zone*. Bull. Geol. Soc. Greece, **XLIII**, 2064-2074.
- Karakostas V., Papadimitriou E., Mesimeri M., Gkarlaouni Ch. and Paradisopoulou P.; 2014: *The 2014 Cephalonia doublet ( $M_w$  6.1 and  $M_w$  6.0), central Ionian Islands, Greece: seismotectonic implications along the Cephalonia Transform Fault Zone*. In: Proc. 2<sup>nd</sup> Eur. Conf. Earthquake Eng. and Seismol., Istanbul, Turkey, p. 7218.

- Karakostas V., Papadimitriou E., Mesimeri M., Gkarlaoui Ch. and Paradisopoulou P.; 2015: *The 2014 Cephalonia doublet (Mw 6.1 and Mw 6.0) central Ionian Islands, Greece: Seismotectonic implications along the Cephalonia Transform Fault Zone*. Acta Geophys., **63**, 1-16, doi: 10.2478/s11600-014-0227-4.
- Kassaras I., Kazantzidou-Firtinidou D., Ganas A., Tonna S., Pomonis A., Karakostas Ch., Papadatou-Giannopoulou Ch., Psarris D., Lekkas E. and Makropoulos K.; 2018: *On the Lefkas (Ionian Sea) November 17, 2015  $M_w = 6.5$  earthquake macroseismic effects*. J. Earthquake Eng., 31 pp., doi: 10.1080/13632469.2018.1488776.
- Kaviris G., Fountoulakis I., Spingos I., Millas Ch., Papadimitriou P. and Drakatos G.; 2018: *Mantle dynamics beneath Greece from SKS and PKS seismic anisotropy study*. Acta Geophys., **66**, 1341-1357.
- Kiratzi A.A. and Langston C.; 1991: *Moment tensor inversion of the January 17, 1983 Kefallinia event of Ionian Islands*. Geophys. J. Int., **105**, 529-535.
- Melnick D., Bookhagen B., Echtler H.P. and Strecker M.R.; 2006: *Coastal deformation and great subduction earthquakes, Isla Santa Maria, Chile (37° S)*. Geol. Soc. Am. Bull., **118**, 1463-1480, doi: 10.1130/B25865.1.
- Okada Y.; 1985: *Surface deformation due to shear and tensile faults in a half-space*. Bull. Seismol. Soc. Am., **75**, 1135-1154.
- Papadimitriou E.E.; 1993: *Focal mechanism along the convex side of the Hellenic Arc and its tectonic significance*. Boll. Geof. Teor. Appl., 35, 401-426.
- Papadimitriou E.E.; 2002: *Mode of strong earthquake occurrence in central Ionian Islands (Greece). Possible triggering due to Coulomb stress changes generated by the occurrence of previous strong shocks*. Bull. Seismol. Soc. Am., **92**, 3293-3308.
- Papadimitriou E., Karakostas V., Mesimeri M., Chouliaras G. and Kourouklas, Ch.; 2017: *The Mw 6.7 17 November 2015 Lefkada (Greece) earthquake: structural interpretation by means of aftershock analysis*. Pure Appl. Geophys., doi: 10.1007/s00024-017-1601-3.
- Papazachos B.C. and Papazachou C.C.; 2003: *The earthquakes of Greece*. Ziti Publication Co., Thessaloniki, Greece, 304 pp.
- Patias P., Georgiadis Ch., Anzidei M., Kaimaris D., Pikridas Ch., Mallinis G., Doumaz F., Bosman A., Sepe V. and Vecchie A.; 2018: *Coastal 3D mapping using very high resolution satellite images and UAV imagery: new insights from the SAVEMEDCOASTS project*. In: Proc. SPIE 10773, Sixth International Conference on Remote Sensing and Geoinformation of the Environment (RSCy2018), 107730V, doi: 10.1117/12.2325540.
- Pizzimenti L., Brunori C.A., Doumaz F., Anzidei M., Serpelloni E., Vecchio A., Patias P., Georgiadis Ch., Kaimaris D., Pikridas Ch., Trivigno M.L., Greco M., Michetti M., Torresan S. and Terranova C.; 2018: *Relative sea level rise by 2100 and flooding hazard along the coastal plains of the Mediterranean region: new insights from the SAVEMEDCOASTS project*. In: Proc. 20<sup>th</sup> EGU General Assembly, Vienna, Austria, p. 14950.
- Sakellariou D., Zavitsanou A., Tsampouraki-Kraounaki K. and Rousakis G.; 2018: *The interplay between active tectonics and sea-level fluctuations and their impact on the evolution of the prehistoric landscapes in the Aegean Region*. In: Abstracts 2<sup>nd</sup> Scientific Meeting of Tectonics Committee of Geological Society of Greece, Patras, Greece.
- Sakkas V. and Lagios E.; 2017: *Ground deformation effects from the ~ M 6 earthquakes (2014 - 2015) on Cephalonia - Ithaca Islands (western Greece) deduced by GPS observations*. Acta Geophys., **65**, 207-222.
- Scordilis E.M., Karakaisis G.F., Karakostas B.G., Panagiotopoulos D.G., Comninakis P.E. and Papazachos B.C.; 1985: *Evidence for transform faulting in the Ionian Sea: the Cephalonia Island earthquake sequence*. Pure Appl. Geophys., **123**, 388-397.
- Steketee J.A.; 1958: *On Voltera's dislocations in a semi-infinite elastic medium*. Can. J. Phys., **36**, 192-205.
- Waldhauser F.; 2001: *HypoDD - a program to compute double-difference hypocenter locations*. U.S. Geological Survey, Menlo Park, CA, USA, Open File Report 01-113, 25 pp.
- Waldhauser F. and Ellsworth W.L.; 2000: *A double-difference earthquake location algorithm: method and application to the Northern Hayward Fault, California*. Bull. Seismol. Soc. Am., **90**, 1353-1368.
- Wessel P., Smith W.H.F., Scharroo R., Luis J.F. and Wobbe F.; 2013: *Generic mapping tools: improved version released*. EOS Trans AGU, **94**, 409-410.

Corresponding author: Eleftheria Papadimitriou  
 Geophysics Department, School of Geology, Aristotle University of Thessaloniki  
 University Campus, GR54124 Thessaloniki, Greece  
 Phone: +30 231 0998488; e-mail: ritsa@geo.auth.gr